İSTANBUL UNIVERSITY
CERRAHPAŞA

ORIGINAL ARTICLE
Electrica 2023; 23(2): 357-365

Evaluating Electromagnetic Interference for Fault Analysis and Maintenance in New Energy Vehicles

Quancheng Wu, Zhongguo You, Jiansong Li, Ting Wu, Lin Luo

Department of Mechanical and Electrical Engineering, Nanchong Vocational and Technical College, Nanchong, Sichuan,China

Cite this article as: Q. Wu, Z. You, J. Li, T. Wu and L. Luo, "Evaluating electromagnetic interference for fault analysis and maintenance in new energy vehicles," *Electrica*, 23(2), 357-365, 2023.

ABSTRACT

To study the electromagnetic compatibility of energy vehicles, the conducted electromagnetic interference (EMI) prediction model of a motor drive system under no-load state is established. The occurrence of EMI in each component of an electric vehicle is discussed along with some mitigation techniques. Further, an EMI filter topology using an LC filter is demonstrated, and the procedure has been verified in two switching power supply control applications. The simulation value of the differential mode interference voltage prediction model is essentially the same as the measured value in the transmitted interference frequency band. Except for a few frequency points, the error is small in most frequency bands, which is about 15%. The values of common mode current simulation and the measured values of the predicted model are essentially the same in the frequency range studied, and the error is about 8% within the allowable range. The horizontal and vertical components of the 10-m electric field on the right side of the car body were modeled in the high-frequency structure simulator program and compared with the results measured in a half-wave anecogenic chamber. The electric field amplitude is basically consistent and can reach approximately 80%, which confirms the accuracy of the vehicle radiation EMI simulation hypothesis.

***Index Terms*—**Electromagnetic interference, motor drive system, new energy vehicles, prediction model.

I. INTRODUCTION

In order to overcome the conflict between fuel supply, demand, and environmental pollution, the world's major automakers have made the development of new energy vehicles (NEVs) a national strategy [1]. To this end, in 2001, our country launched the "863 National Program of the Tenth Five-Year Plan, a major project of electric vehicles." The implementation of the NEV production access management rules in 2007 marks that China has officially encouraged the development of NEVs and promoted their industrialization [2]. In March 2012, the "Twelfth Five-Year Plan for the Development of Electric Vehicle Technology" established "clean electricity" as the main technical road, and then in July, the State Council adopted the "Energy Saving and New Energy Vehicle" Industrial Development Plan (2012). By 2020, the total production and sales of pure electric cars and plug-in hybrid electric vehicles are expected to exceed 5 million [3].

With the continuous advancement of science and technology and the continuous development of the automotive industry, people's demands for car economy, safety, and comfort are increasing. Electric vehicle is the fusion product of "electrification" and "automobile." Compared with ordinary vehicles, the increase of its electrical and electronic equipment leads to the centralized layout of various types of electrical and electromagnetic equipment. Vehicle control, communication, and navigation equipment are connected together through electrical equipment. The frequency of electromagnetic wave ranges from tens of hertz to megahertz, forming an extremely complex electromagnetic environment. Therefore, the electromagnetic compatibility of electric vehicles cannot be ignored [4].

GB/T4365-2003 defines the term electromagnetic compatibility as "the ability of a device or system to function normally in its own electromagnetic environment without interfering with the electromagnetic interference of anything in the environment" [5]. In terms of vehicle electromagnetic compatibility, this means that the entire vehicle, parts, or individual technical parts can operate normally in an electromagnetic environment without excessive electromagnetic

Corresponding author:
Quancheng Wu

E-mail: wuquancheng7@126.com

Received: July 8, 2022

Accepted: November 13, 2022

Publication Date: March 30, 2023

DOI: 10.5152/electrica.2023.22120

interference (EMI) with anything in the environment [6]. That is, in the car and its surrounding space, under the condition of available spectrum resources, the car itself and the surrounding equipment can coexist without degradation. The harsh electromagnetic environment inside the narrow space of electric vehicle leads to the increasingly serious EMI between the electronic equipment in the vehicle, resulting in the problem of EMI. The result may weaken the function of the interfered electrical equipment or seriously reduce the function of the equipment, resulting in unimaginable vehicle operation accidents. In the face of such a harsh electromagnetic environment inside the electric vehicle, how to reduce the mutual interference of a variety of electronic and electrical equipment in the car, improve the anti-interference of electrical equipment, and ensure the safe operation of equipment has become an important topic in the research of electric vehicle technology [7].

Another crucial component of NEVs is the electric powertrain systems, which combine traction motors and motor controllers with gears, clutches, and other mechanical components. The e-powertrain drastically simplifies the structure and propulsion of the vehicle, and its topologies have a significant impact on the performance of NEVs [8].

Because of this, the requirements for the electric drive systems in NEVs primarily focus on the following aspects: 1) high torque density and good torque control capability for vehicle dynamic performance; 2) reliability and durability for the necessary vehicle safety and life; and 3) excellent performance-to-cost ratio for the energy economy and users' capital investment as well as high efficiency within the operation spectrum [9]. There is a summary of the technology involved with traction motors, their power electronic controllers, and electric powertrains. For the benefit of researchers and engineers working on NEV powertrain systems, the merits and cons of the current technology, as well as their future possibilities, are highlighted. The rest of article is organized as follows: the most recent work in the field of EMI fault analysis and maintenance is presented in Section II. The adopted methodology is presented in Section III which is followed by the results and discussion in Section IV. At last, the conclusion is discussed in Section V.

II. LITERATURE REVIEW

The power system of electric vehicles is different from that of traditional vehicles. A high-voltage motor drive system is used as the power source of vehicles. High dv/dt and di/dt switching characteristics of power devices in the system, such as changes in traction motor speed or torque, create high-amplitude, broadband EMI, affecting the safety and intelligence of the system. Systems, control systems, and other devices that are vulnerable to EMI pose a hidden threat to the safety of electric vehicles [10]. Fig. 1 is the structure diagram of the motor drive system of a hybrid electric vehicle. The system is mainly composed of a high-voltage power battery, converter, drive motor, and its corresponding control circuit. The rated voltage of the battery is 144 V and the rated power is 18 kW. The output power of the power battery is different according to the different working conditions of the vehicle. When the converter works, the voltage at both ends of insulated-gate bipolar transistor (IGBT) can reach 150 V. In the starting state, the current change on the power line can be as high as 60 A. Therefore, the motor drive system is considered as a high-voltage and high-current system, which is easy to affect the normal operation of other surrounding electrical systems [11].

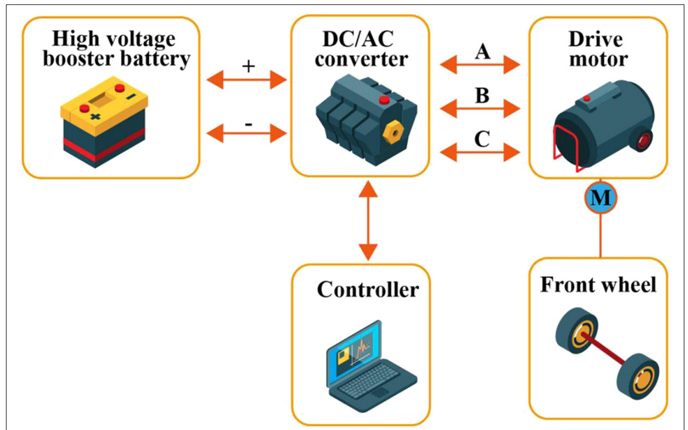

Fig. 1. Structure diagram of a motor drive system.

Electro Magnetic Compati (EMC) studies of motor drive systems are particularly important in solving the EMC problems of electric vehicles:

1) The voltage level of the power battery is high. When the motor drive system works normally, the IGBT will form steep pulses with large amplitude, which will produce EMI with a wide frequency band and large energy. It is the main interference source in the vehicle [12].
2) The EMI generated by the system will propagate to the surrounding through the power line, load connection line, and control signal line and be coupled to other electronic devices. The coupling process involves conduction and radiation, which directly affects the distribution of electromagnetic environment inside and outside the vehicle [13].
3) The EMI from the engine's steering system is strong, which is an important factor affecting the safe and reliable operation of electric vehicles. It is one of the important reasons why it is difficult to pass the relevant EMC certification standards [14].

With the large increase of on-board electrical equipment, the problem of automotive electromagnetic compatibility is becoming more and more prominent. Many developed countries and international organizations in the world have put forward EMI and EMS standards for automotive products and formed a complete set of vehicle EMC system, which is mainly reflected in having perfect vehicle EMC standards, accurate EMC testing system and effective vehicle EMC testing, and management and certification institutions. Many countries have developed EMC prediction, analysis, and design software for large vehicles and have continuously developed new materials, new processes, and new products suitable for vehicle EMC control technology [15]. China's automobile electromagnetic compatibility technology started late, and the overall capacity of research, development, and production is still basically in the primary stage [16]. In recent years, with the increasing frequency of China's automobile foreign trade, the state and automobile manufacturers began to pay attention to the EMC problem of automobiles, and the electromagnetic compatibility laboratory has sprung up [10]. At present, the research on EMC of an electric vehicle motor drive system mainly focuses on three aspects: component-level modeling, system-level model establishment, and interference suppression [17]. The component-level modeling of a motor drive system mainly focuses on the research of switching devices and passive devices. The modeling of switching devices is mainly to establish the electronic circuit model based on the physical characteristics of semiconductors. For example, some researchers have established the piecewise linear behavior model of IGBT. This method does not require one to know the specific physical structure of IGBT. The model parameters can be obtained by measuring and consulting the IGBT data table [18]. On the whole, a lot of research has been carried out in the field of automotive EMC, some results have been achieved, and a series of industry standards have been formulated. The research idea is basically to solve practical problems through simulation modeling and experimental verification of specific research objects or using experiments to guide the establishment of simulation models [19]. In China, this aspect started late, and there are few studies, especially in the research of EMC of an electric vehicle motor drive system. At present, there are some problems in the research on EMC of an electric vehicle motor drive system at home and abroad, such as how to establish high-precision and broadband motor model. The modeling of converter switching devices is too complex to study the conducted interference under various working conditions and establish its interference prediction simulation model. It is also difficult to build the body model, deal with the electrical size, and model the interference source [20].

The two separate EMI filtering techniques utilized to address the conducted interference caused by the high-voltage power supply of the DC–DC converter have been examined by Singh *et al.* [21]. The design of a wideband EMI filter for high-voltage ports is followed by the design of an EMI filter at the Printed Circuit Board (PCB) level to reduce the resonance frequency. Effective filter was selected and put into place to lessen the conducted interference after the findings were compared. In their study of the EMI in power converter design, Zhang *et al.* [22] also showed the Metal-Oxide-Semiconductor Field-Effect Transistor (MOSFET) and diode's frequency domain characteristics expressed in the time domain. In Khamitov *et al.*'s [23] study, interference suppression techniques for electric car motor driving systems, charging systems, and low voltage systems are discussed. Shielding techniques are presented along with the primary EMI sources that were observed. In order to demonstrate how EMI is induced in the wireless charging port and to address the occurrence of transients and EMI concerns in the system, Emori *et al.* [24] have examined the switching transients in the EV charging system. Xiong *et al.* [25] presented a methodology in which an impedance balance is used as a filtering unit as opposed to the traditional way, which uses an active and passive filter and decreases the system's efficiency through heat loss.

III. RESEARCH METHODS

A. Conducted Electromagnetic Interference Experimental Platform of a Motor Drive System Under Different Working Conditions

In order to build an experimental platform that can simulate various working conditions of the system, two key equipment need to be used: power cabinet and electric dynamometer [26]. The experimental layout diagram of a pure electric vehicle motor drive system is shown in Fig. 2, which mainly includes power battery test and simulation equipment, Line Impedance Stabilization Network (LISN), connecting cable, DC/AC converter, three-phase cable, permanent magnet synchronous motor, electric dynamometer, and supporting equipment.

B. Introduction to Conductor Electromagnetic Radiation

Each module of the motor drive system uses wires for physical connection. The higher the electromagnetic energy or signal frequency transmitted by the wires, the more obvious the wire antenna effect. Therefore, the radiation EMI problem of the whole system can be attributed to the electromagnetic radiation problem of the wires, which can usually be regarded as the radiation emission of the wire antenna. The wire antenna can be regarded as composed of countless electric dipoles. As long as the correct current distribution on the wire antenna can be obtained, the electromagnetic field around the wire can be obtained by using the integral of the electromagnetic field generated by the unit electric dipole in the surrounding space [27].

The spherical coordinate system should be used to discuss the antenna radiation. According to the electromagnetic radiation theory, when the electric dipole is placed at the origin of the spherical coordinate, the spherical coordinate component of the electromagnetic field at any point in space is as shown in (1), (2), and (3).

$$dE_r = \frac{2Idlk^3\cos\theta}{4\pi\omega\varepsilon_0}\left[\frac{1}{(kr)^2} - \frac{j}{(kr)^3}\right]e^{-jkr} \tag{1}$$

$$dE_\theta = \frac{Idlk^3\sin\theta}{4\pi\omega\varepsilon_0}\left[\frac{j}{kr} + \frac{1}{(kr)^2} - \frac{j}{(kr)^3}\right]e^{-jkr} \tag{2}$$

$$dH_\phi = \frac{Idlk^2\sin\theta}{4\pi}\left[\frac{j}{(kr)} + \frac{1}{(kr)^2}\right]e^{-jkr} \tag{3}$$

where $k = 2\pi f\sqrt{\mu_0\varepsilon_0}$ is the phase constant (f is the frequency, ε_0 is the dielectric constant of free space, and μ_0 is the permeability) and r is the radial distance from the observation point to the origin [28].

The following model is based on the electromagnetic radiation EMI model of current-carrying conductor. Assuming that the conductor is oriented along the z-axis, the length is L, and the cross-section is ignored, the conductor is divided into electric dipole composed

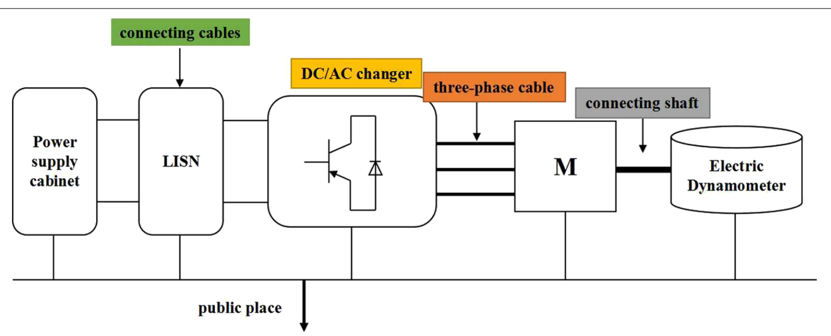

Fig. 2. Schematic diagram of a motor drive system.

of an infinite number of element current segments. The element field strength generated by the electric dipole Idz' at z' at the observation point P can be directly obtained from (1)–(3) and from (4) and (5).

$$\begin{aligned} dE &= dE_r\boldsymbol{e}_r + dE_\theta\boldsymbol{e}_\theta \\ &= \frac{2Idz'k^3\cos\theta'}{4\pi\omega\varepsilon_0}\left[\frac{1}{(kR)^2}-\frac{j}{(kR)^3}\right]e^{-jkR}\boldsymbol{e}_r \\ &+\frac{Idz'k^3\sin\theta'}{4\pi\omega\varepsilon_0}\left[\frac{j}{kR}+\frac{1}{(kR)^2}-\frac{j}{(kR)^3}\right]e^{-jkR}\boldsymbol{e}_\theta \end{aligned} \tag{4}$$

$$\begin{aligned} dH &= dH_\phi\boldsymbol{e}_\phi \\ &= \frac{Idz'k^2\sin\theta'}{4\pi}\left[\frac{j}{kR}+\frac{1}{(kR)^2}\right]e^{-jkR}\boldsymbol{e}_\phi \end{aligned} \tag{5}$$

In the formula, $R=\left|r-z'e_z\right|$ is the radial distance from the electric dipole Idz' to the observation point P, and $\boldsymbol{e}_r$, $\boldsymbol{e}_\theta$, and $\boldsymbol{e}_\phi$ are the unit vectors in the directions of r, θ, and ϕ, respectively [29].

According to the trigonometric function expression, $\sin\theta'=\frac{|r|}{R}\sin\theta$ and $\cos\theta'=\frac{|r|\cos\theta-z'}{R}$. The electromagnetic field generated by the conductor current I at point P is the superposition of the electromagnetic field generated by all electric dipoles on the conductor at point P, that is, (6) and (7).

$$\begin{aligned} E &= \int_L dE \\ &= \int_L\left(\frac{Ik^4}{2\pi\omega\varepsilon_0}\cdot\left(|r|\cos\theta-z'\right)\left[\frac{1}{(kR)^3}-\frac{j}{(kR)^4}\right]e^{-jkR}\right)dz'e_r \\ &+\int_L\left(\frac{Ik^4}{4\pi\omega\varepsilon_0}\cdot|r|\sin\theta\left[\frac{j}{(kR)^2}+\frac{1}{(kR)^3}-\frac{j}{(kR)^4}\right]e^{-jkR}\right)d'\boldsymbol{e}_\theta \end{aligned} \tag{6}$$

$$=\int_L d\boldsymbol{H}=\int_L\left(\frac{Ik^3}{4\pi}\cdot|\boldsymbol{r}|\sin\theta\left[\frac{j}{(kR)^2}+\frac{1}{(kR)^3}\right]e^{-jkR}\right)dz'\boldsymbol{e}_\phi \tag{7}$$

It can be seen from (6) and (7) that the electromagnetic field generated by the conductor can be calculated when the current distribution on the conductor is known.

C. Finite Element Model of Electric Vehicle Body

The structure of electric vehicle is complex, the number of components or parts is huge, the geometric characteristics of various components are complex, the size difference is great, and the spatial distribution is uneven. Therefore, it is not enough to use only one software to establish the finite element model of vehicle body [30, 31]. In this paper, CATIA, HyperMesh, HFSS, and other software are jointly used to establish the HFSS finite element analysis model for the car body. The modeling process is shown in Fig. 3.

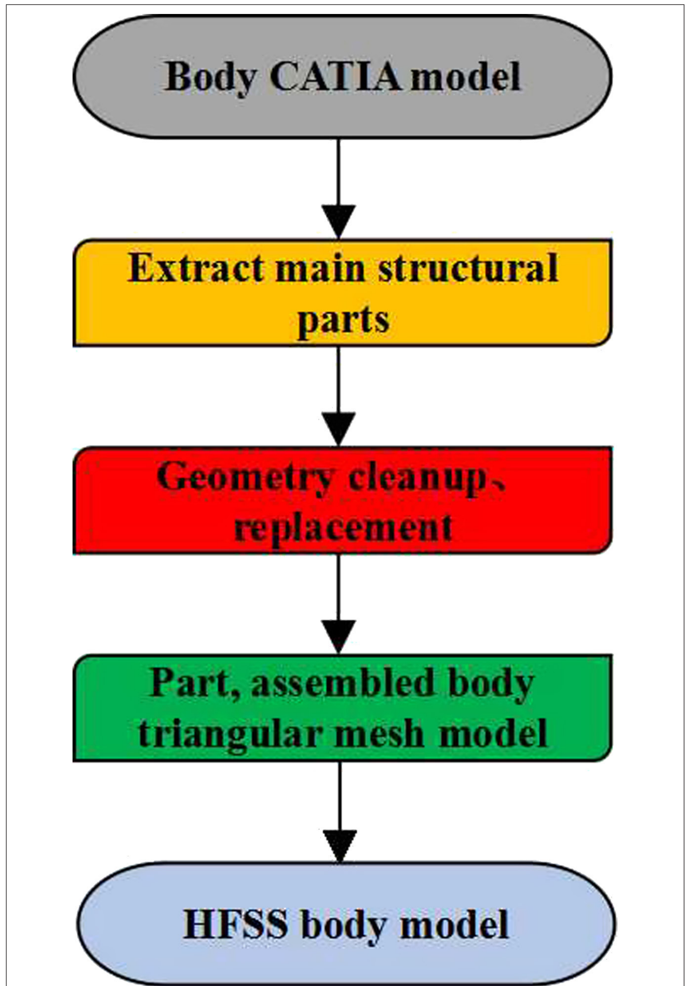

Fig. 3. Finite element model modeling process of a car body.

IV. RESULT ANALYSIS

A. Simulation Analysis of Conducted Electromagnetic Interference of a Motor Drive System

An EMI hypothesis model based on the experimental platform, as well as a common mode and differential mode interference hypothesis model, was developed in accordance with the proposed method for creating an EMI simulation circuit model for a motor steering system, which uses a circuit model based on the method of adjusting the permission vector. Two operating conditions for the drive system were selected as the object of study. These two operating conditions are simulated and alternated. The spectra of the common mode external current on the three-phase cable at the end of the DC/AC output are also compared with the test results.

Fig. 4 is a comparative diagram of the common mode external voltage simulation and the actual measurement on the LISN under two operating conditions. This shows that the modeled and measured values of the common mode external voltage spectrum on the LISN in the two operating conditions as a whole in the intermittent frequency band (100 kHz–30 MHz) are well matched, especially in the range of 400 kHz–30 MHz. The fact that the amplitude error of the mode voltage is less than 5 dB indicates that the predicted model has high-frequency characteristics. For the no-load and 45 states, the simulation and measurement errors are large in the low-frequency range of 100 kHz–400 kHz, especially at the initial frequency; the error is up to 10 dB. On a few frequency points (2 MHz), the error reaches 20 dB. For the reverse charging state, the error between the simulation and measured values of the whole frequency band is less than 5 dB.

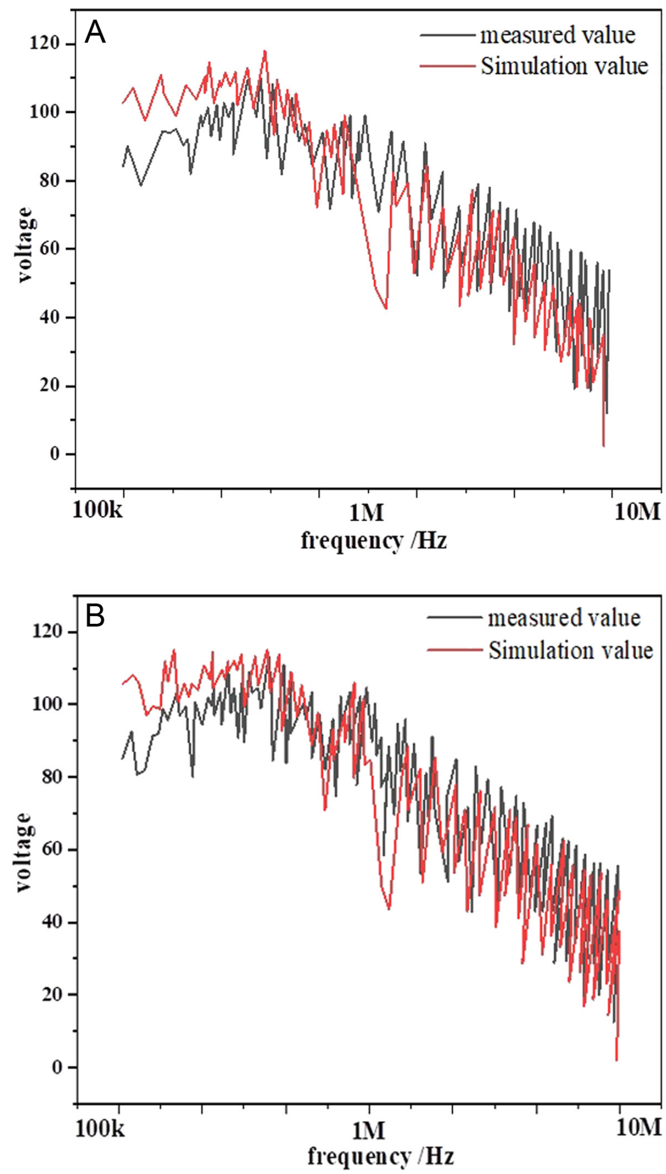

Fig. 4. Comparison between LISN common mode voltage simulation and measurement.

Comparing the measured common mode interference voltage spectrum in Fig. 4(a) and (b), it can be found that the change trend of the common mode interference voltage spectrum tested on the drive system LISN is basically the same under the two states. On the whole, the spectrum amplitude of the common mode interference voltage in 45 and reverse charging states is greater than that in the no-load state. The voltage spectrum amplitude in the 45 state is slightly higher than that in no-load state in most frequency bands, while that in reverse charging state is about 10 dB higher than that in the no-load state in almost the whole frequency band. This is because under different working conditions of the motor drive system, the amplitude of the common mode interference source is different, and the common mode conducted interference current flowing through each module in the system is different: the larger the amplitude of the interference source is, the larger the interference current flowing through each module when the common mode impedance of each part remains unchanged. 45 and reverse charging conditions, the amplitude of system interference source is larger than that in no-load state, and the common mode interference current is also larger. Therefore, the spectrum amplitude of common mode interference voltage coupled to LISN is also larger.

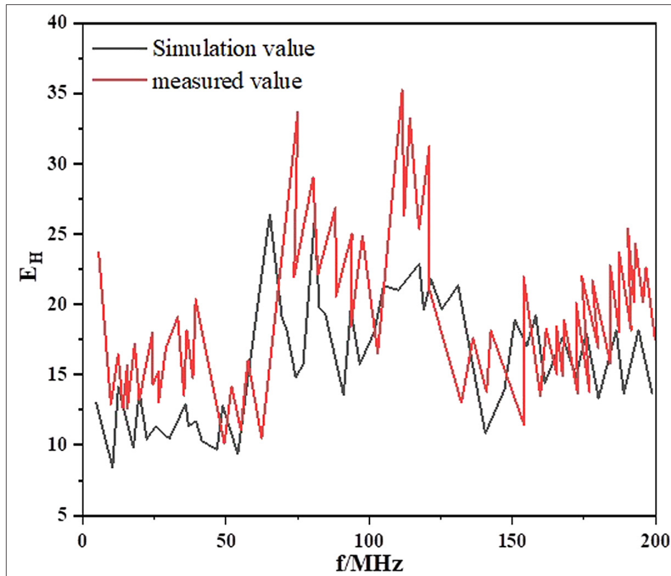

Fig. 5. Test results and simulation results of the horizontal component of electric field intensity.

B. Electromagnetic Radiation Model Simulation Experiment of a Motor Drive System

In the experiment of electromagnetic radiation EMI driven by a motor, the vehicle is fixed on the turntable, the front wheel of the vehicle is located on the hub, and the vehicle speed is stabilized at 40 km/h to ensure that the power conversion system is in the non-working state. The radiated EMI of the electric vehicle is measured.

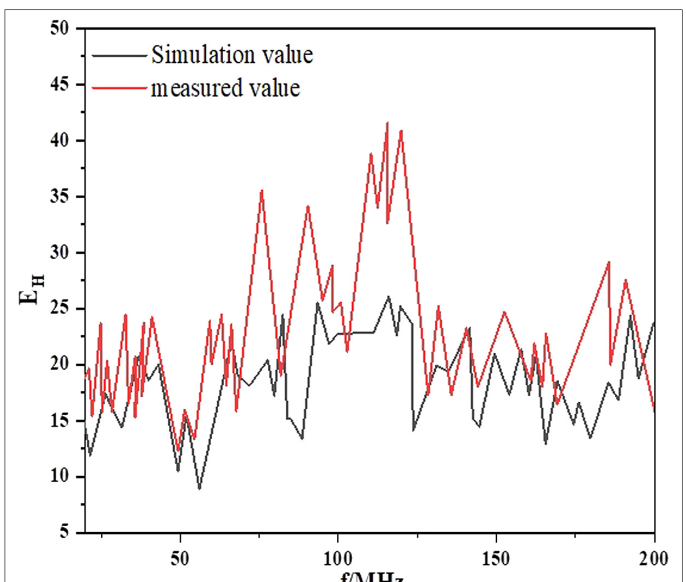

Fig. 6. Test results and simulation results of the vertical component of electric field intensity.

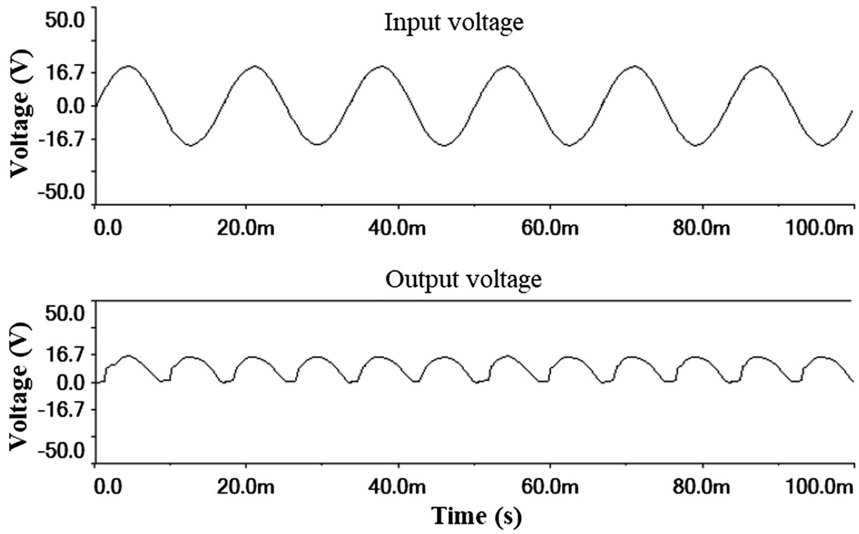

Fig. 7. Outcomes of the proposed model with electromagnetic interference filter topology.

The receiving antenna is located 10 m to the right of the vehicle body and the electric field is 3 m in the horizontal direction (positive direction of the *x*-axis) and 3 m in the vertical direction (positive direction of the *z*-axis). The frequency range of the test is 30–200 MHz. Take a point every 0.05 MHz, say a total of 3401 frequency points. The simulation and test results of the horizontal and vertical components of the electric field are shown in Figs. 5 and 6, respectively.

It can be seen from Figs. 5 and 6 that the electric field amplitude of the motor drive system in the horizontal and vertical directions of the test point 10 m away is basically consistent with the variation law with the frequency in the range of 30–200 MHz. The amplitude of the actual measured value is larger than that of the simulation as a whole, and the amplitude difference can reach 20 dB at some frequency points. In addition, the common mode radiated current is not only included in the actual radiated current measurement of the electric power supply but also the EMI generated by the common mode radiated current is excluded in the actual measurement process.

When the EMI filter is added to the circuit, the results of the circuit model demonstrate unequivocally that harmonics are totally eliminated, as seen in Fig. 7. When the EMI filter is not incorporated into the circuit, the results produced for the circuit model clearly demonstrate the presence of harmonics, as seen in Fig. 8. The findings of the study make it abundantly evident that the main sources of EMI are the motor windings and the switching of power switches. Additionally, it has been found that EMI signals can quickly propagate via cables or space via radiation, having an impact on both the electromagnetic environment and the conditions in which electric vehicles operate.

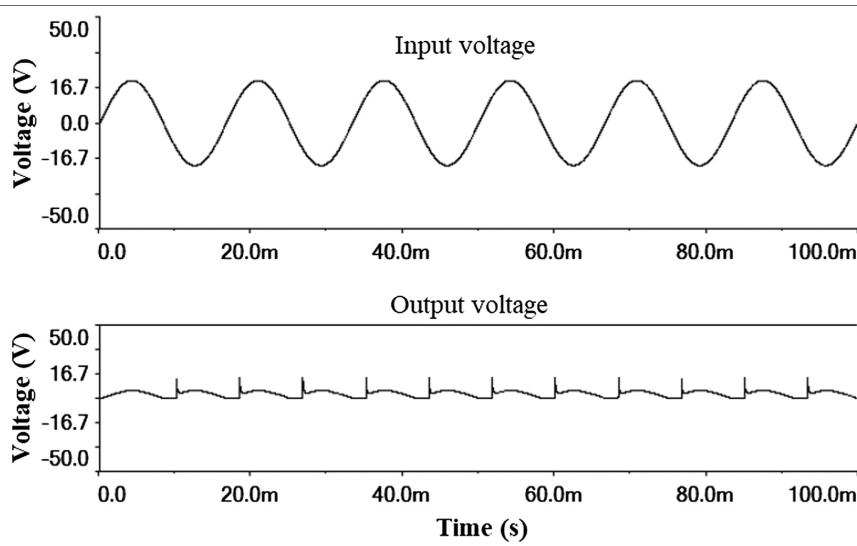

Fig. 8. Outcomes of the proposed model without electromagnetic interference filter topology.

V. CONCLUSION

The research work of this paper studies the electromagnetic compatibility of the electric vehicle motor drive system. To sum up the full text, the work and main achievements of this paper are as follows:

1) The EMI in the engine system identifies the source and distribution path. Based on the principle of operation of the engine system, it is analyzed that the rapid rise/fall of the terminal voltage of the main circuit switching device will produce a great impact, which is the main reason for the EMI of the system. When the frequency and duty cycle of trapezoidal wave remain unchanged, the spectrum characteristics of trapezoidal wave are studied when the voltage amplitude and rise/fall time change. It is concluded that the greater the voltage amplitude and the shorter the rise/fall time, the greater the spectrum amplitude. The EMI generated during the operation of the DC/AC converter was identified as the main source of interference in the motor drive system, and the distribution path of EMI in the motor drive system was analyzed.
2) The use of the EMI prediction model of the engine steering system under various operating conditions was analyzed. This document builds a test platform for a pure electric vehicle engine steering system that can meet a variety of actual operating conditions to test the predictability of a predictive model. Grounded EMI data (voltage and current). Simultaneously, an EMI prediction model of the three operating conditions of the motor drive system was installed in the Saber software to calculate the common mode interference voltage, differential mode interference voltage, and three-phase cable. The results show that the EMI prediction model of the engine steering system is effective. The modeling method in this article is very versatile and portable.
3) The EMI model of vehicle radiation in the engine steering system is being studied. In accordance with the requirements of GB18655 national standard, electromagnetic radiation test was performed on the motor drive system, and the 30–200 MHz frequency range was defined as the radiation interference study frequency band of the motor drive system. The electromagnetic radiation mechanism of the telephone is analyzed, and the radiated electromagnetic interference model of the steering system is established. Various software connection processing technologies use the CATIA model of the electric vehicle body as a simplified and limited element model horizontal and vertical component. The intensity of the 10-m electric field on the right side of the vehicle body was modeled by the HFSS software and compared with the results measured in a half-wave anecogenic chamber.

In future work, the radiation EMI model of a vehicle's engine system can be used to accurately predict the electromagnetic compatibility of an electric vehicle's radiation.

Peer-review: Externally peer-reviewed.

Author Contributions: Concept – Q.W.; Design – L.L.; Supervision – T.W.; Materials – T.W.; Data Collection and/or Processing – J.L.; Analysis and/or Interpretation – J.L.; Literature Review – Q.W.; Writing – Z.Y.; Critical Review – Z.Y.

Declaration of Interests: The authors have no conflicts of interest to declare.

Funding: The authors declared that this study has received no financial support.

REFERENCES

1. X. Chen, S. Leng, J. He, and L. Zhou, "Deep learning based intelligent inter-vehicle distance control for 6g-enabled cooperative autonomous driving," *IEEE Internet Things J.*, vol. PP, no. 99, pp. 1–1, 2020.
2. Y. Wu, Y. Xu, J. Zhou, Z. Wang, and H. Wang, "Research on starting control method of new-energy vehicle based on state machine," *Energies*, vol. 13, no. 23, p. 6249, 2020. [CrossRef]
3. Wu, Z. Zhang, Li, and Q. Sun, "Open-circuit fault diagnosis of six-phase permanent magnet synchronous motor drive system based on empirical mode decomposition energy entropy," *IEEE Access*, vol. 99, pp. 91137–91147, 2021.
4. Y. Tang, Y. He, F. Wang, G. Lin, and R. Kennel, "A centralized control strategy for grid-connected high-speed switched reluctance motor drive system with power factor correction," *IEEE Trans. Energy Convers.*, vol. 36, no. 3, pp. 2163–2172, 2021.
5. Y. Zhu, H. Wu, and C. Zhen, "Regenerative braking control under sliding braking condition of electric vehicles with switched reluctance motor drive system," *Energy*, vol. 230, no. 7, p. 120901, 2021.
6. D. Terazono, J. Liu, Y. Miura, S. Sakabe, H. Bevrani, and T. Ise, "Grid frequency regulation support from back-to-back motor drive system with virtual-synchronous-generator-based coordinated control," *IEEE Trans. Power Electron.*, vol. 36, no. 3, pp. 2901–2913, 2021. [CrossRef]
7. Z. F. Zhang, Y. Wu, and S. Y. Qi, "Diagnosis method for open-circuit faults of six-phase permanent magnet synchronous motor drive system," *IET Power Electron.*, vol. 13, no. 15, pp. 3305–3313, 2020. [CrossRef]
8. Z. Quan, L. Ge, Z. Wei, Y. W. Li, and L. Quan, "A survey of powertrain technologies for energy-efficient heavy-duty machinery," *Proc. IEEE*, vol. 109, no. 3, pp. 279–308, 2021. [CrossRef]
9. M. Ehsani, Y. Gao, S. Longo, and K. M. Ebrahimi, *Modern Electric, Hybrid Electric, and Fuel Cell Vehicles*. Boca Raton, USA: CRC press, 2018.
10. Y. Mei, and G. Yi, "Advanced model predictive current control for induction motor drive system fed by indirect matrix converter," *J. Power Electron.*, vol. 20, no. 2, pp. 466–478, 2020. [CrossRef]
11. K. Wróbel, P. Serkies, and K. Szabat, "Model predictive base direct speed control of induction motor drive—Continuous and finite set approaches," *Energies*, vol. 13, no. 5, p. 1193, 2020. [CrossRef]
12. Z. Sadeghi, S. M. S. Nejad, A. Rashidi, and M. Shahparasti, "Fast demagnetization and vibration reduction in switched reluctance motor drive system," *IEEE Access*, vol. 9, pp. 110904–110915, 2021.
13. C. Yao, X. Wu, and Y. Z. Zhou, "Fault-tolerant operation control strategy for combined winding bearingless flux-switching permanent magnet motor drive system with one opened phase," *IEEE Trans. Energy Convers.*, vol. 36, no. 4, pp. 2861–2871, 2021.
14. D. Seo, Y. Bak, and K. B. Lee, "An improved rotating restart method for a sensorless permanent magnet synchronous motor drive system using repetitive zero voltage vectors," *IEEE Trans. Ind. Electron.*, vol. 67, no. 5, pp. 3496–3504, 2020. [CrossRef]
15. H. Chen, J. Yang, and S. Xu, "Electrothermal-based junction temperature estimation model for converter of switched reluctance motor drive system," *IEEE Trans. Ind. Electron.*, vol. 67, no. 2, pp. 874–883, 2020. [CrossRef]
16. K. Diao, X. Sun, G. Lei, G. Bramerdorfer, and J. Zhu, "System-level robust design optimization of a switched reluctance motor drive system considering multiple driving cycles," *IEEE Trans. Energy Convers.*, vol. 36, no. 1, pp. 348–357, 2021.
17. Y. F. Jia *et al.*, "Control strategy for an open-end winding induction motor drive system for dual-power electric vehicles," *IEEE Access*, vol. 8, pp. 8844–8860, 2020. [CrossRef]
18. M. Nandakumar, S. Ramalingam, S. Nallusamy, and S. S. Rangarajan, "Hall-sensor-based position detection for quick reversal of speed control in a bldc motor drive system for industrial applications," *Electronics*, vol. 9, no. 7, p. 1149, 2020. [CrossRef]
19. K. Aiso, A. Kan, and Y. Aoyama, "A novel flux-switching magnetic gear for high-speed motor drive system," *IEEE Trans. Ind. Electron.*, vol. 68, no. 6, pp. 4727–4736, 2020.
20. M. Moradighahderijani, and B. M. Dehkordi, "Comprehensive robust and fast control of z-source inverter-based interior permanent magnet synchronous motor drive system," *IEEE Trans. Ind. Electron.*, vol. 68, no. 12, pp. 11783–11793, 2021.

21. A. Singh, A. Mallik, and A. Khaligh, "A comprehensive design and optimization of the DM EMI filter in a boost PFC converter," *IEEE Trans. Ind. Appl.*, vol. 54, no. 3, pp. 2023–2031, 2018. [CrossRef]
22. Y. Zhang, X. Zhang, Y. I. F. U. Ding, and L. Jiang, "Research on electromagnetic compatibility of new energy vehicles," *DEStech Trans. Eng. Technol. Res.*, 2017. [CrossRef]
23. A. Khamitov *et al.*, "Dynamic wireless charging of electric vehicles: Multichannel modeling," In 2018 IEEE International Conference on Environment and Electrical Engineering and 2018 IEEE Industrial and Commercial Power Systems Europe (EEEIC/I&CPS Europe). IEEE Publications, 2018, pp. 1–5. [CrossRef]
24. K. Emori, J. Niida, A. Okubo, K. Numakura, T. Hayashi, and T. Hara, "SiC inverter for electric vehicles with improved trade-off between reduced switching losses and increased radiation noise," In 2019 IEEE Energy Conversion Congress and Exposition (ECCE). IEEE Publications, 2019, pp. 4058–4062. [CrossRef]
25. Y. Xiong *et al.*, "An electric drive system modelling method based on module behavior," In 2019 International Conference on Microwave and Millimeter Wave Technology (ICMMT), IEEE Publications, 2019, pp. 1–3. [CrossRef]
26. P. Otomański, E. Pawowski, and A. Szlachta, "The evaluation of expanded uncertainty of dc voltages in the presence of electromagnetic interferences using the LabVIEW environment," *Meas. Sci. Rev.*, vol. 21, no. 5, pp. 136–141, 2021. [CrossRef]
27. J. Baranowski, T. Drabek, P. Piątek, and A. Tutaj, "Diagnosis and mitigation of electromagnetic interference generated by a brushless dc motor drive of an electric torque tool," *Energies*, vol. 14, no. 8, p. 2149, 2021. [CrossRef]
28. Y. Zhang, S. Wang, and Y. Chu, "Analysis and comparison of the radiated electromagnetic interference generated by power converters with si mosfets and gan hemts," *IEEE Trans. Power Electron.*, vol. 35, no. 8, 2020. [CrossRef]
29. G. Mier Escurra, A. Rodrigo Mor, and P. Vaessen, "Influence of the pulsed voltage connection on the electromagnetic distortion in full-size hvdc cable pea measurements," *Sensors (Basel)*, vol. 20, no. 11, p. 3087, 2020. [CrossRef]
30. H. Chen, T. Wang, S. Ye, and T. Zhou, "Modeling and suppression of electromagnetic interference noise on motor resolver of electric vehicle," *IEEE Transactions on Electromagnetic Compatibility*, vol. 63, no. 3, pp. 720–729, 2021.
31. Z. Zhang, and T. Su, "Behavioral analysis and immunity design of the ro-based trng under electromagnetic interference," *Electronics*, vol. 10, no. 11, p. 1347, 2021. [CrossRef]

Quancheng Wu (January 1985), male, the Han nationality, lecturer, research area: automobile maintenance and new energy vehicle technology. At present, he is working in Nanchong Vocational and Technical College.

Zhongguo You (April 1984), male, the Han nationality, lecturer, research area: automobile maintenance and new energy vehicle technology. At present, he is working in Nanchong Vocational and Technical College.

Jiansong Li (May 1993), male, the Han nationality, master degree, lecturer, research area: engine emission control and vocational education. At present, he is working in Nanchong Vocational and Technical College.

Ting Wu (November 1989), female, the Han nationality, assistant, research area: vehicle inspection and maintenance technology. At present, she is working in Nanchong Vocational and Technical College.

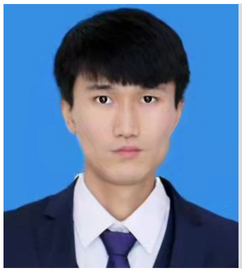

Lin Luo (December 1992), male, the Han nationality, master degree, research area: dynamic characteristics of hybrid electric vehicles. At present, he is working in Nanchong Vocational and Technical College.